J Mater Sci (2007) 42:8350–8356
DOI 10.1007/s10853-006-0764-6

Fabrication of TiC and TiB_2 locally reinforced steel matrix composites using a Fe–Ti–B_4C–C system by an SHS-casting route

Zhiqiang Zhang · Ping Shen · Yan Wang · Yunpeng Dong · Qichuan Jiang

Received: 27 April 2006 / Accepted: 7 August 2006 / Published online: 22 June 2007

Abstract Steel matrix composites locally reinforced by in situ TiC and TiB_2 particulates were successfully fabricated using self-propagating high-temperature synthesis (SHS) in a Fe–Ti–B_4C–C system during casting. The locally reinforced steel matrix composites consist of three distinct regions: (i) a TiC and TiB_2 particulate-reinforced region, (ii) a transition region, and (iii) a steel matrix region. The TiC and TiB_2 particulates in the locally reinforced regions display a relatively uniform distribution, and their sizes decrease with the increase in Fe content from 10 wt.% to 40 wt.%. The wear resistance of the locally reinforced region of the steel matrix composites is much higher than that of the unreinforced steel matrix.

Introduction

Over the past decades, the incorporation of ceramic reinforcements into steel or iron matrix to produce composites with improved wear resistance has been extensively investigated [1–16], since they possess combined properties of toughness and machinability related to the conventional steel or iron, and high hardness and good wear resistance related to the ceramic. Among various ceramic particulates, titanium carbide and titanium diboride are potential materials because of their outstanding properties such as high hardness, low density, high melting temperature, high modulus, excellent wear and corrosion resistance [6, 7, 17] and good wettability and stability in steel melt compared with other ceramics [18]. Therefore, they are widely used as the reinforcements in the steel- or iron-matrix composites.

There are various routes to fabricate the TiC or TiB_2 reinforced steel- or iron-matrix composites such as powder metallurgy [1–3], conventional casting [4–7], carbothermic reduction [8–10], self-propagating high-temperature synthesis (SHS) [11–15] and aluminothermic reduction [16]. Among which, SHS is an especially promising technique due to its high productivity and low cost, eliminating the requirement of complex equipment for producing the ceramic reinforced composites. Also, the materials fabricated by SHS are generally of high purity, i.e., free from absorption, oxidation and detrimental interface reaction, leading to a strong interfacial bond between the matrix and the reinforcements [11, 13, 17].

Unfortunately, most of the TiC or TiB_2 particulates reinforced steel- or iron-matrix composites in the previous researches were of monolithic nature, i.e., the ceramic reinforcements were homogeneously distributed in the entire body of the matrix. In the practical applications, however, only local part undergoes severe abrasion. The materials, especially the reinforcements, and the production cost are thus greatly wasted if a monolithically reinforced composite is employed. In this respect, the authors attempt to produce the locally reinforced steel matrix composites using an SHS-casting route, and have successfully fabricated the TiC or/and TiB_2 particulates locally reinforced steel matrix composites using Al–Fe–Ti–B, Al–Ti–B_4C and Ni–Ti–B_4C systems [19–21]. The general procedure could be described as follows: the molten steel preheated to 1,873 K was poured into a sand mould

Z. Q. Zhang · P. Shen · Y. Wang · Y. P. Dong · Q. C. Jiang (✉)
Key Laboratory of Automobile Materials, Ministry of Education, and Department of Materials Science and Engineering, Jilin University, No.5988 Renmin Street, Changchun 130025, P.R. China
e-mail: jqc@jlu.edu.cn

where the reactant preforms were preplaced and fixed using locating pins. The surface region of the preform was rapidly heated by the high-temperature steel melt and the reactants were ignited, creating a combustion wave, which propagate from the surface to the center of the preforms. The main characteristic of this method is that the sample is ignited from all directions of the surface, not just from one direction. This is somewhat different from the conventional SHS and thermal explosion modes. The detailed microstructures in the locally reinforced composites, however, were not elaborated in the previous studies [19–21].

Additionally, in our previous studies [19, 20], it was found that when aluminum was used as the reactant to promote the reaction it could evaporate during the reaction due to high exotherm of the SHS reaction, resulting in many pores in the solidified samples. Therefore, aluminum has a detrimental effect on the property of the composites. In this study, we select a Fe–Ti–B_4C–C system to fabricate the TiC–TiB_2 particulates reinforced steel matrix composites based on the following considerations: firstly, the melting temperature of Fe is relatively high, which could alleviate the reaction exotherm to a great extent, and Fe is the primary element in the steel compositions; secondly, the combined TiC and TiB_2 particulates in the composites are expected to provide a better reinforcing effect on the wear resistance of the locally reinforced region; and finally, the incorporation of C in the system will increase the content of TiC in the reaction products and produce the composites with 50%TiC–50%TiB_2 (by molar fraction) which are expected to provide better mechanical properties [22].

Experimental

The starting materials of the preforms were commercial powders of Fe (98.5 wt.% purity, ~5 μm), Ti (99.5 wt.% purity, ~15 μm), B_4C (95.0 wt.% purity, ~3.5 μm) and C (99.9 wt.% purity, ~38 μm). For preparing the TiC and TiB_2 reinforced steel matrix composites, the powders in compositions for the formation of TiC: TiB_2 = 1:1 in molar ratio with 10, 20, 30 and 40 wt.% Fe were mixed in a stainless-steel container for 7 h, and then were pressed into cylindrical preforms with dimensions of ~20 mm in diameter and 15 mm in height using a stainless steel die with two plungers. The green densities of the preforms were estimated to be 62 ± 2% of theoretical, as determined by the mass and geometry measurements.

A low Cr alloy steel was selected as the matrix for the composites. Table 1 gives its compositions. Four green preforms were pre-placed in a sand mould before casting, as schematically illustrated in Fig. 1 of Ref. [21]. The steel was first melted at about 1,873 K in a 5 kg medium frequency induction furnace, and then poured into the sand mould. The SHS reaction in the Fe–Ti–B_4C–C preforms was initiated by the heat of the liquid steel.

Table 1 Compositions of the steel matrix (wt.%)

C	Si	Mn	Cr	Ni	Ti	S	P	Fe
0.27	0.18	0.21	1.01	0.01	0.03	0.02	0.02	Bal.

After cooling in the sand mould, the locally reinforced steel matrix composites were taken out, sectioned and polished. Microstructures were analyzed using scanning electron microscopy (SEM) (Model JSM-6310LV, Japan) and energy-dispersive X-ray microanalysis (EDAX). Phases were identified by X-ray diffraction (XRD) (Model D/Max 2500PC Rigaku, Japan). The sliding abrasive wear was tested under a load of 35 N using a pin-on-disc apparatus. Both the steel matrix and the reinforced composites were cut into specimens with 6 mm in diameter and 15 mm in height and used as pin materials, while 360-mesh SiC abrasive paper was used as the counterface.

Results and discussion

Adiabatic temperature

The TiC and TiB_2 particulates could be synthesized by the following reaction:

$$x\mathrm{Fe} + 4\mathrm{Ti} + \mathrm{B_4C} + \mathrm{C} \rightarrow x\mathrm{Fe} + 2\mathrm{TiC} + 2\mathrm{TiB_2} \qquad (1)$$

where x is the Fe content in the Fe–Ti–B_4C–C system ranging from 10 wt.% to 40 wt.%. The reaction enthalpy, ΔH, at 298 K was calculated to be –944.33 kJ/mol using the thermodynamic data from Ref. [23], indicating that the reaction is high-exothermic. Since the enthalpies of the reactants and products are commonly given at 298 K, and the propagating mode is often initiated at room temperature without any preheat, the adiabatic temperature in this reaction system could be theoretically calculated using the following equation [24]:

$$\Delta H(298) + \int_{298}^{T_{ad}} \sum n_j C_p(P_j)\mathrm{d}T + \sum_{298-T_{ad}} n_j L(P_j) = 0 \qquad (2)$$

where $\Delta H(298)$ is the reaction enthalpy at 298 K, $C_p(P_j)$ and $L(P_j)$ are the heat capacity and latent heat of the products, T_{ad} is the adiabatic temperature, and P_j and n_j refer to the product and the mole fraction, respectively. The necessary thermodynamic data [23] for the calculation are shown in Table 2.

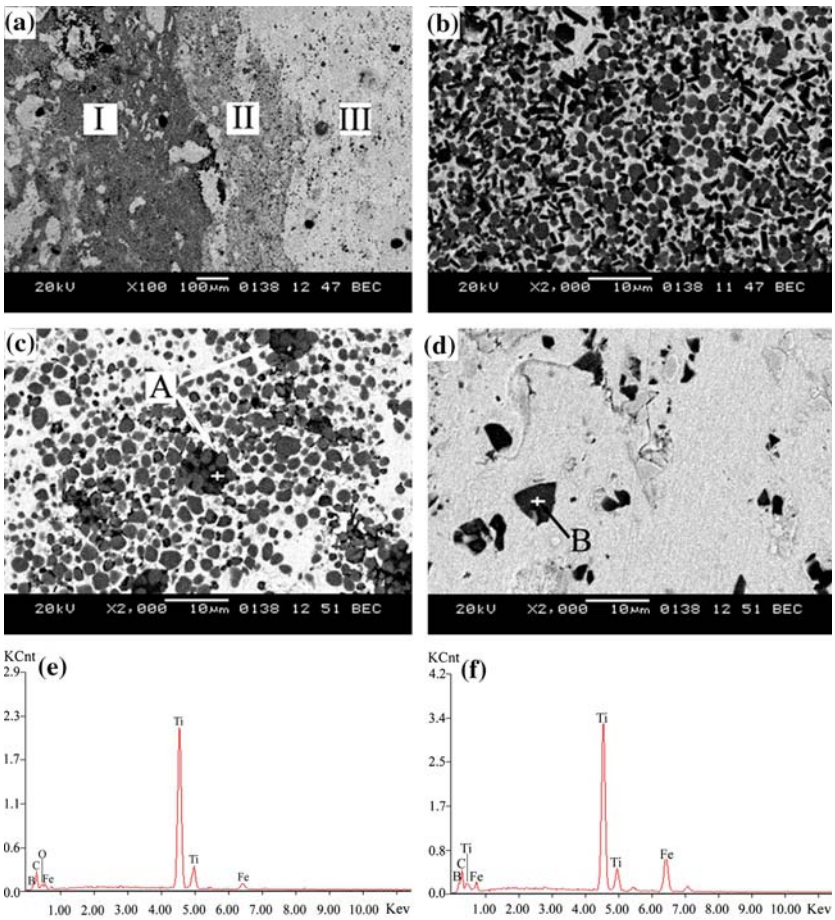

Fig. 1 (**a**) Back scattered electron images of the TiC and TiB_2 locally reinforced steel composites with 30 wt.% Fe in the reactants in a low magnification; (**b**–**d**) high magnification micrographs of region (i), region (ii) and region (iii), respectively; and (**e**) and (**f**) EDAX analysis on positions marked by symbols ''+''

Table 2 Thermodynamic data of TiC, TiB_2 and Fe [23]

Property (units)		Data
TiC	$T_{m,\ TiC}$ (K)	3,290
	$\Delta H^0_{f(298\ K)}$(kJ mol^{-1})	–184.10
	C_{p1} (J.K^{-1} mol^{-1})	$49.953 + 0.979*10^{-3}T - 14.774*10^{5}T^{-2} + 1.887*10^{-6}T^{2}$
	$\Delta H_{m,TiC}$(kJ mol^{-1})	71.13
TiB_2	$T_{m,\ TiB2}$ (K)	3,193
	$\Delta H^0_{f(298\ K)}$(kJ mol^{-1})	–323.84
	C_{p2} (J K^{-1} mol^{-1})	$56.379 + 25.857*10^{-3}T - 17.464*10^{5}T^{-2} - 3.347*10^{-6}T^{2}$
	$\Delta H_{m,\ TiB2}$ (kJ mol^{-1})	100.42
Fe	$T_{m,\ Fe}$ (K)	1,809
	C_{p3} (J K^{-1} mol^{-1})	$28.175 - 7.318*10^{-3}T - 2.895*10^{5}T^{-2} + 25.041*10^{-6}T^{2}$ (298 K–800 K)
		$-263.454 + 255.810*10^{-3}T + 619.232*10^{5}T^{-2}$ (800 K–1000 K)
		$-641.905 + 696.339*10^{-3}T$ (1000 K–1042 K)
		$1946.255 - 1788.335*10^{-3}T$ (1042 K–1060 K)
		$-561.932 + 334.143*10^{-3}T + 2912.114*10^{5}T^{-2}$ (1060 K–1184 K)
		$23.991 + 8.360*10^{-3}T$ (1184 K–1665 K)
		$24.635 + 9.904*10^{-3}T$ (1665 K–1809 K)
		46.024 (1809 K–3135 K)
		27.062 (3135 K–3600 K)
	$\Delta H_{m,\ Fe}$ (kJ mol^{-1})[a]	13.81
	$\Delta H_{b,\ Fe}$ (kJ mol^{-1})[b]	349.57
B_4C	$\Delta H^0_{f(298\ K)}$(kJ mol^{-1})	–71.55

[a] subscript m represents ''melting''

[b] subscript b represents ''boiling''

Table 3 The adiabatic temperatures of the Fe-Ti-B_4C-C system with different Fe contents.

Fe content (wt.%)	Adiabatic temperature (K)
10	3,135
20	3,135
30	3,000
40	2,715

Table 3 shows the calculated adiabatic temperatures, T_{ad}, for the Fe–Ti–B_4C–C system with 10, 20, 30 and 40 wt.% Fe. Clearly, the values of T_{ad} decrease with the increase in Fe content; however, they are all higher than 1,800 K, indicating that the reaction could be self-sustaining according to Merzhanov's empirical criterion [24]. Also, the adiabatic temperatures are much higher than the melting temperatures of Fe (1,812 K) and Ti (1,948 K), and the maximum combustion temperature for the preform with 40 wt.% Fe was measured to be 2,128 K without preheating treatment [Zhang, unpublished work], indicating that the Fe and Ti powders as well as their intermetallics in the preform would be in a molten state after the high-exothermic reaction was initiated.

Microstructure

Figure 1 shows the representative microstructures in the locally reinforced steel matrix composite developed from a Fe–Ti–B_4C–C preform with 30 wt.% Fe. It can be seen that the composite consists of three distinct regions: (i) a TiC and TiB_2 particulate reinforced region, (ii) a transition region and (iii) a matrix region. In the reinforced region, there are two kinds of particulates in view of their appearance. The dark-gray particulates with hexagonal prism or rectangular shapes are TiB_2, and the bright-gray ones with a round shape are TiC. The shapes of these particulates are typical and similar to those of the monolithic TiB_2 and TiC phases synthesized from Al–Ti–B [25] and Al–Ti–C systems [26]. In addition, the bright regions are rich in Fe, which may partly come from the reactants and partly from the steel. Because the wettability of both TiC and TiB_2 by Fe is quite good [18], the molten steel can spontaneously penetrate into the pores of the reacted products by the capillary force after the SHS reaction, and develop good bonds with the particulates.

The formation of the transition region is favorable to alleviate the stress between the reinforced region and the matrix, which is expected to improve the fracture toughness of the composites. In this region, only the TiC particulates were observed in this region [see Fig. 1(c)], whose sizes are similar to those in region (i). The reasons for only the TiC particulates formation might be as follows: (1) the diffusion rate of carbon in titanium is much higher than that of boron [27, 28], and there are much carbon in the reactants of the Fe–Ti–B_4C–C system as well as in the steel melt, as a result, the concentration of carbon in the transition region is much higher compared to that of boron; and (2) because the maximum temperature of the combustion synthesis reaction is much higher than the melting temperature of Ti (1,948 K), the titanium powders in the outer layer of the preform would melt and mix with the molten steel around the preform, which reacted with carbon, leading to the formation of the TiC particulates.

Also, it was observed that in regions (ii) and (iii), there are some black large particulates as marked by letters 'A' and 'B' in Fig. 1. EDAX demonstrates that they are $Ti(C,B)_x$ phases with a small amount of Fe. This may be attributed to the reactants, particularly for the B_4C powders at the edge of the sample falling off and being entrained into the steel matrix after the molten steel was poured into the mould and the reaction was initiated. As seen from the appearance, the origin of those particulates in the two regions seems to be similar, i.e., from B_4C with size ~3.5 μm.

Figure 2 shows the SEM microstructures in the TiC and TiB_2 locally reinforced regions of the composites with 10, 20, 30, and 40 wt.% Fe in the reactants. The TiC and TiB_2 particulates in the locally reinforced regions exhibit a relatively uniform distribution. Furthermore, it can be clearly seen that the size of TiC and TiB_2 particulates decreases with the increase in Fe content from 10 wt.% to 40 wt.%. The reasons are that the real combustion temperature decreases as the Fe content increases and the growth of the reaction product is an exponential function of the combustion temperature [23]. The relationship between the crystal growth rate, k, and temperature, T, is given by the Arrhenius equation [29]

$$k = A\exp(-E/RT) \tag{3}$$

where A is the surface area of the crystal, E is the activation energy for the crystal growth, and R is the universal gas constant. According to Eq. (3), with the decrease in combustion temperature as a result of the increase in Fe in the reactants, the TiC and TiB_2 crystal growth rate decreases. Also, the increased liquid metals surrounding the TiC and TiB_2 grains reduce the tendency for them to coalescence, and prevent their sintering to form larger grains. Furthermore, some pores were also observed in the microstructures. The formation of the pores results mainly from the evaporation of the adsorbed gas, volatilization of some impurities, and the volume shrinkage between the reactants and products after the SHS reaction.

Figure 3 shows the XRD patterns of the TiC and TiB_2 locally reinforced regions of the steel matrix composites with 10, 20, 30 and 40 wt.% Fe in the reactants. It can be

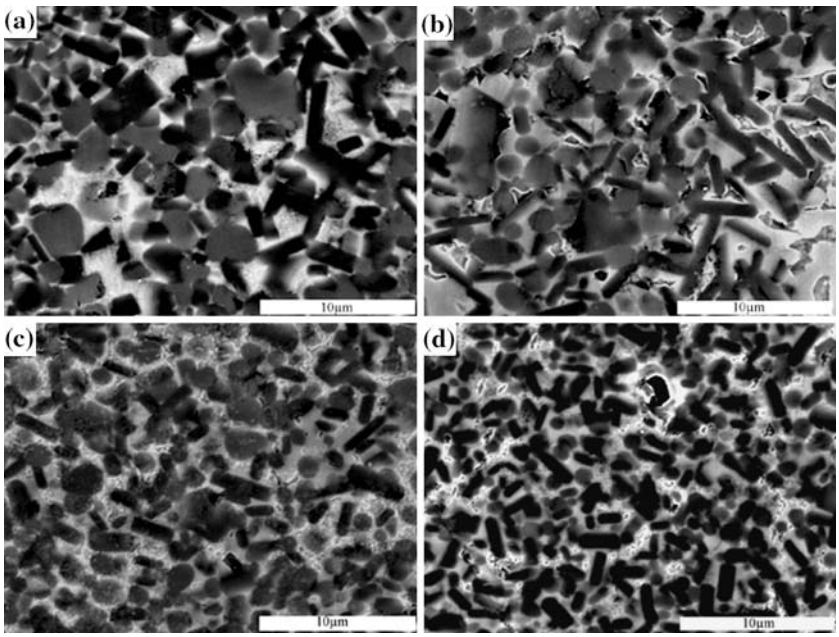

Fig. 2 Microstructures in the TiC and TiB_2 reinforced steel matrix regions with (**a**) 10; (**b**) 20; (**c**) 30; and (**d**) 40 wt.% Fe in the reactants, respectively

seen that the phases in the synthesized steel matrix composites consist of Fe, TiC, TiB_2 and a small amount of Fe_2B phase. The reason for the formation of the Fe_2B phase in the composites might be the reaction between Fe and TiB_2 in the presence of carbon, as suggested by Degnan et al. [7].

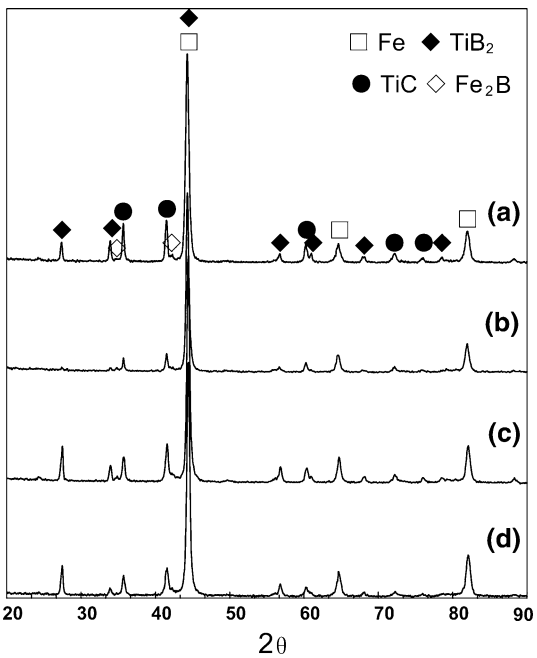

Fig. 3 XRD patterns of the composites with (**a**) 10; (**b**) 20; (**c**) 30 and (**d**) 40 wt.% Fe in the reactants, respectively

Wear resistance

Figure 4 shows the volumetric wear loss rates of the unreinforced steel and the TiC and TiB_2 locally reinforced composites with 10, 20, 30 and 40 wt.% Fe in the reactants. The results indicate a great reduction in the abrasive wear loss rate of the steel by the incorporation of the ceramic particulate reinforcements. The reason for improving the wear resistance is that the TiC and TiB_2 particulates bear the load [6]. The in situ TiC and TiB_2 particulates possess high hardness, therefore they can blunt the abrasive SiC particulates and reduce the metal matrix to contact SiC during sliding. On the other hand, the interfacial bonds between both the TiC and TiB_2 particulates and the steel

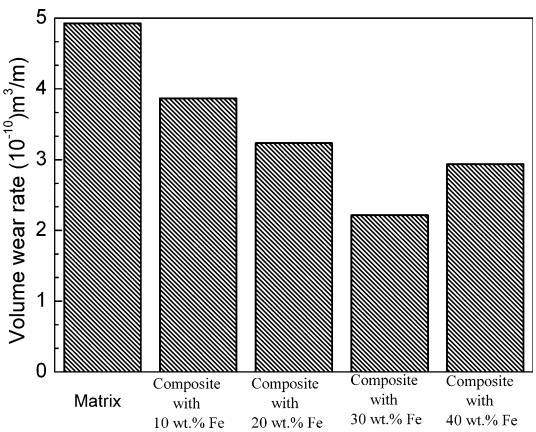

Fig. 4 Volume wear rates of the unreinforced steel and locally reinforced composites with different Fe contents in the reactants

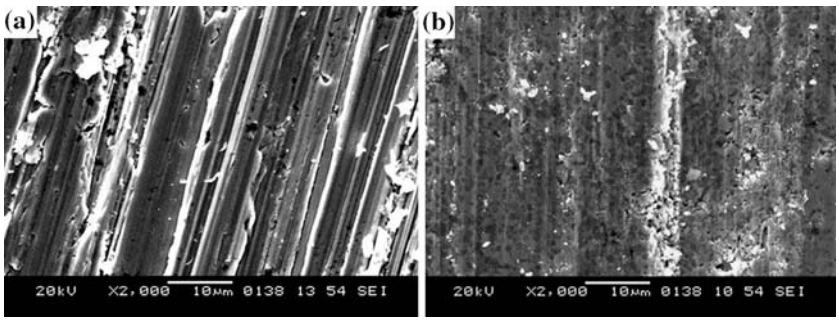

Fig. 5 The worn surface morphology of (**a**) the unreinforced steel and (**b**) the TiC and TiB_2 reinforced composite with 40 wt.% Fe in the reactants

matrix are estimated to be strong in light of the good wettability between the ceramics and the steel matrix [18], which can prevent the particulates spalling from the matrix during the wear tests, consequently improving the wear performance.

It is interesting to note that the TiC and TiB_2 particulates reinforced composite with 30 wt.% Fe in the reactants shows the lowest volume wear rate, which is almost twice lower than that of the unreinforced steel. The best wear resistance of the composites with 30 wt.% Fe in the reactants could be attributed to:

(1) The quantity of pores in the reinforced regions with 10 wt.% and 20 wt.% Fe in the reactants is more than that with 30 wt.% Fe, because the former two have higher reaction temperatures. The wear loss of the composites with 10 wt.% and 20 wt.% Fe in the reactants comes mainly from poorly bonded areas, where pores exist.
(2) With the increase in Fe content from 30 wt.% to 40 wt.%, the quantity of the TiC and TiB_2 particulates decreases, and so does the hardening effect. Therefore, the reinforced region of the composite with 30 wt.% Fe in the reactants has a better wear resistance.

Figure 5 shows the typical morphology of the worn surface. As can be seen, there are a lot of deep and narrow grooves on the worn surface of the unreinforced steel matrix, as the SiC abrasive particulates plough across the surface, remove and push the material to the sides of the grooves. However, the amount of groove is substantially less on the worn surface of the TiC and TiB_2 reinforced region, and the grooves are shallow and wide, as shown in Fig. 5b. Due to strong interfacial bond and good compatibility between the in situ synthesized particulates and the steel matrix, there is no severe pullout or de-adhesion of the particulates from the steel matrix. Some reinforced particulates are exposed to the worn surface of the composite, which blunt the abrasive SiC particulates and reduce the subsequent wear loss.

Conclusions

(1) In situ TiC and TiB_2 particulates locally reinforced steel matrix composites were successfully fabricated by the SHS reactions in the Fe–Ti–B_4C–C system with 10, 20, 30 and 40 wt.% Fe, respectively, in the molten steel during casting.
(2) The locally reinforced steel matrix composites consist of three distinct regions: (i) the TiC and TiB_2 particulate reinforced region, (ii) the transition region and (iii) the matrix region. The TiC and TiB_2 particulate sizes in the reinforced regions decrease with the increase in Fe content from 10 wt.% to 40 wt.% in the reactants.
(3) The wear resistance of the locally reinforced regions is significantly higher than that of the unreinforced steel, which increases by 27–122%, depending on the Fe content in the reactants, after the incorporation of the TiC and TiB_2 particulate reinforcements.

Acknowledgements This work is supported by The National Natural Science Foundation of China (no.50531030) and The Ministry of Science and Technology of the P.R. China (no. 2005CCA00300) as well as The Project 985-Automotive Engineering of Jilin University.

References

1. Pagounis E, Lindroos VK (1998) Mater Sci Eng A246:221
2. Pagounis E, Talvitie M, Lindroos VK (1996) Metall Mater Trans A 27A:4171
3. Tjong SC, Lau KC (2000) Compos Sci Technol 60:1141
4. Raghunath C, Bhat MS, Rohatgt PK (1995) Scripta Mater 32:577
5. Doğan ÖN, Hawk JA (1995) Scripta Mater 33:953
6. Degnan CC, Shipway PH (2002) Wear 252:832
7. Degnan CC, Shipway PH (2002) Metall Mater Trans A 33A:2973
8. Brown IWM, Owers WR (2004) Curr Appl Phys 4:171
9. Terry BS, Chinymakobvu OS (1991) J Mater Sci Lett 10:628
10. Chen Y (1997) Scripta Mater 36:989
11. Saidi A, Chrysanthou A, Wood JV (1994) J Mater Sci 29:4993
12. Capaldi MJ, Saidi A, Wood JV (1997) ISIJ Inter 37:188
13. Saidi A, Chrysanthou A, Wood JV, Kellie JLF (1997) Ceramics Inter 23:185
14. Fan QC, Chai HF, Jin ZH (1999) J Mater Sci 34:115

15. Fan QC, Chai HF, Jin ZH (2001) J Mater Sci 36:5559
16. Bandyopadhyay TK, Chatterjee S, Das K (2004) J Mater Sci 39:5735
17. Das K, Bandyopadhyay TK, Das S (2002) J Mater Sci 37:3881
18. Li RJ (2004) Ceramic-metal composites. Metallurgical Industry Press, Beijing (In Chinese)
19. Jiang QC, Wang Y, Wang HY, Ma BX, Zhang ZQ (2004) ISIJ Inter 44:1847
20. Jiang QC, Ma BX, Wang HY, Wang Y, Dong YP (2005) Compos Part A 37:133
21. Wang HY, Huang L, Jiang QC (2005) Mater Sci Eng A407:98
22. Brodkin D, Zavaliangos A, Kalidindi SR, Barsoum MW (1999) J Am Ceram Soc 82(3):665
23. Liang YJ, Che YC (1993) Data handbook of inorganic thermodynamics. Northeastern University Press, Shenyang (In Chinese)
24. Moore JJ, Feng HJ (1995) Prog Mater Sci 39:243
25. Jiang QC, Li XL, Wang HY (2003) Scripta Mater 48:713
26. Wang HY, Jiang QC, Zhao YQ, Zhao F, Ma BX, Wang Y (2004) Mater Sci Eng A372:109
27. Laskar AL, Bocquet JL, G. Brebec, Monty C (1990) Diffusion in materials. Kluwer, Dordrecht
28. Brodkin D, Kalidindi SR, Barsoum MW, Zavaliangos A (1996) J Am Ceram Soc 79(7):1945
29. Mullin JW (2001) Crystallization. Butterworth-Heinemann, Oxford